

$$E \sim n\Phi_0 H \varphi^2 S,$$

where n is the concentration of vortices, Φ_0 is the magnetic flux quantum, H is the magnetic field, φ is the angle of inclination of the vortex structure to the direction of the magnetic field, and S is the cross sectional area of the cell perpendicular to the vortex filaments. This energy can be regarded as the product of the generalized coordinate φ and the generalized force $\sim n\Phi_0 HS \varphi$. Then experiments with rotation of the magnetic field can be treated as the deformation of the vortex lattice (change in the generalized coordinate φ under the action of the generalized force). The value of the force here is connected with the concentration of the pinning centers through the area S . The greater S the fewer the pinning centers and the greater the force. The observed results can easily be treated here as the plastic deformation of the vortex lattice—the formation of dislocation half loops from the surface of the sample. The combination of such half loops leads to the turning of the pinned part of the vortex lattice in the direction

of the acting force. The greater the dimensions of the cell S , the greater the deviation. The irreversibility here is natural. The results given in Fig. 6 for a sample without the memory effect can be treated as deformation hardening due to the crossing of the vortex filaments upon formation and motion of the dislocations as a consequence of the deviation of the magnetic field and its return to the previous direction.

- ¹B. Monceau, D. Saint-James and Q. Waysand, *Phys. Rev. B* **12**, 3673 (1975).
- ²A. Ya. Vin'kov, O. V. Zharikov, Ch. V. Kopetskaĭ and V. M. Polovov, *Fiz. Nizkikh Temp.* **3**, 11 (1977) [*Sov. J. Low Temp. Phys.* **3**, 4 (1977)].
- ³V. A. Somenkov, V. R. Petrunin, S. Sh. Shil'shteĭn and A. A. Chertkov, *Kristallogr.* **14**, 617 (1969) [*Sov. Phys. Crystallogr.* **14**, 522 (1969)].
- ⁴S. A. Govorkov and V. A. Tul'ın, *Zh. Eksp. Teor. Fiz.* **70**, 1044 (1976) [*Sov. Phys. JETP* **43**, 545 (1976)].
- ⁵I. Milne, *Phil. Mag.* **28**, 133 (1973).

Translated by R. T. Beyer

Experimental and theoretical investigation of spin-reorientation phase transitions in cubic ferromagnets and ferrimagnets in a magnetic field

V. G. Bar'yakhtar, V. A. Borodin, V. D. Doroshev, N. M. Kovtun, R. Z. Levitin, and E. P. Stefanovskii

Donets Physico-technical Institute, Ukrainian Academy of Sciences, USSR
(Submitted 7 July 1977)
Zh. Eksp. Teor. Fiz. **74**, 600–619 (February 1978)

A theoretical investigation of the nature of the spin-flip phase transitions inducible by a magnetic field in infinite cubic ferromagnets is carried out with allowance for the fourth- and sixth-order terms in the expression for the magnetic-anisotropy energy. Possible (H, T) orientational phase diagrams corresponding to magnetic-field directions along high-symmetry axes of the type $\langle 100 \rangle$, $\langle 111 \rangle$, and $\langle 110 \rangle$ are constructed. The critical points of the first-order phase transitions are determined, and the transitional domain structure accompanying a first-order transition in samples of finite dimensions is studied. An experimental verification of the results of the theory has been carried out on single crystals of the rare-earth iron garnets $Tb_x Y_{3-x} Fe_5 O_{12}$ ($x = 0.10, 0.26$) and $Sm_3 Fe_5 O_{12}$. Some (H, T) phase diagrams have been reproduced on the basis of torque, magnetization, and differential susceptibility studies. Particular attention has been paid to the detection and investigation by the Fe^{57} -NMR method of the transitional domain structure accompanying first-order orientation transitions, as illustrated by the iron garnet $Tb_{0.1} Y_{2.9} Fe_5 O_{12}$.

PACS numbers: 75.30.Kz, 75.50.Bb, 75.50.Gg, 76.60.—k

INTRODUCTION

Considerable attention is being paid at present to the investigation of magnetic phase transitions of the order-order type and, in particular, of spin-flip phase transitions (SFPT). It should be noted that the most intensively investigated SFPT are those occurring in uniaxial and biaxial magnetic substances, especially in the rare-earth orthoferrites (see, for example, the review published in Ref. 1). The study of the cubic ferro- and ferrimagnetic substances began only recently, the main attention having been paid to the investigation of spontaneous SFPT, which occur in zero magnetic field, and

which are due to the change that occurs in the nature of the magnetic crystallographic anisotropy when the temperature changes.^[2-8]

The influence of an external magnetic field on the behavior of the magnetization of an anisotropic cubic ferromagnetic substance in a narrow range of temperatures in the vicinity of the magnetic-ordering temperature has been investigated without allowance for the critical fluctuations in Refs. 9 and 10 and with allowance for the fluctuations in Ref. 11. However, the present authors do not know of any work in which a sufficiently complete analysis has been performed of the orientation phase di-

agrams of anisotropic cubic ferromagnetic substances in the low-temperature limit ($T \ll T_c$), although separate, uncoordinated experimental data^[12-14] and magnetization-curve computations carried out quite long ago^[12,15-17] for some specific ferromagnets show that field-induced SFPT of both first and second order are realized in cubic ferromagnetic substances.

The present work is devoted to the systematic study of SFPT induced in cubic ferro- and ferrimagnetic substances by a magnetic field and temperature within the framework of the phenomenological approximation for $T \ll T_c$. The nature of SFPT in infinite crystals is investigated. Generalized (H, T) phase diagrams corresponding to H orientations along principal crystallographic directions of the type $\langle 100 \rangle$, $\langle 111 \rangle$, and $\langle 110 \rangle$ are constructed by analytical and numerical methods, and the magnetization curves are classified. The critical points (CP) of the first-order orientation transitions are found, and the limits of applicability of the theory ignoring the order-parameter fluctuations to the study of second-order SFPT are estimated. The estimates show that allowance for the fluctuations is unimportant for any practically realizable mode of approach to the second-order SFPT point.

We theoretically consider the transitional (intermediate) state, i.e., the transitional domain structure (TDS), which arises, as is already well known,^[18,19] during the first-order SFPT in samples of finite dimensions.

An experimental verification of certain results of the theory has been carried out on single crystals of iron garnets of the system $Tb_xY_{3-x}Fe_5O_{12}$ and $Sm_3Fe_5O_{12}$, in which temperature-induced first-order SFPT are observed.^[2,5,6] On the basis of torque, magnetization-curve, low-frequency differential-susceptibility, and ⁵⁷Fe-NMR spectrum measurements, we reproduce some (H, T) phase diagrams of these ferrimagnetic substances and compare them with the theoretical diagrams. The NMR method has, moreover, been used to detect and study the intermediate state associated with first-order SFPT.

I. THEORY OF SFPT IN CUBIC FERROMAGNETS IN A MAGNETIC FIELD

§1. Orientation Phase Diagrams

Let us consider an unbounded cubic ferromagnet located in a magnetic field, H , directed along one of the crystallographic axes of the type $\langle 100 \rangle$, $\langle 111 \rangle$, or $\langle 110 \rangle$. Let us assume that it is uniformly magnetized, i.e., let us ignore the existence of equivalent (degenerate) phases, which inevitably exist in a real cubic magnetic substance because of its polyaxial nature when the field is oriented along a high-symmetry direction. For example, if $H \parallel \langle 100 \rangle$ and the easy axes are the $\langle 111 \rangle$ directions, then after the completion of the boundary-shift processes the rotation of the magnetization will begin to occur in the four degenerate phases $\Phi_{\langle 111 \rangle}$ corresponding to the four $\langle 111 \rangle$ directions nearest to the chosen $\langle 100 \rangle$ type direction. A similar situation obtains when H is

oriented along a $\langle 111 \rangle$ or a $\langle 110 \rangle$ axis.

Into the expression for the free energy of the unbounded crystal enter the magnetic crystallographic anisotropy energy and the energy of the magnet in the magnetic field. Limiting ourselves to the fourth- and sixth-order terms, we can write the anisotropy energy of a cubic crystal in the form

$$f_A = K_1(T) (\alpha_1^2 \alpha_2^2 + \alpha_2^2 \alpha_3^2 + \alpha_3^2 \alpha_1^2) + K_2(T) \alpha_1^2 \alpha_2^2 \alpha_3^2,$$

where K_1 and K_2 are the first two cubic magnetic anisotropy constants, which are functions of the temperature T (we neglect the field dependence of K_1 and K_2); the α_i are the direction cosines of the magnetization vector M . In the spherical coordinate system whose polar axis coincides with a $\langle 100 \rangle$ -type four-fold axis of the cubic crystal, the total free energy of the unbounded ferromagnet can be represented in the form

$$f_0 = f_A + f_H = |K_2| \left\{ \frac{1}{4} q \sin^2 2\theta + \frac{1}{4} \left(q + \frac{K_2}{|K_1|} \cos^2 \theta \right) \sin^4 \theta \sin^2 2\varphi - h [\sin \theta \sin \theta_H \cos(\varphi - \varphi_H) + \cos \theta \cos \theta_H] \right\}. \quad (1)$$

Here θ and φ , θ_H and φ_H are the polar and azimuthal angles of the vectors M and H respectively. Neglecting the susceptibility of the para-process, we assume that, at $T \ll T_c$, $|M| = M_0 = \text{const}$. We have adopted the notation:

$$h = M_0 H / |K_2|, \quad q = K_1 / |K_2|. \quad (1a)$$

In Ref. 2 it is shown that, in the absence of an external magnetic field, only the phases $\Phi_{\langle 100 \rangle}$, $\Phi_{\langle 111 \rangle}$, and $\Phi_{\langle 110 \rangle}$ are realizable in a cubic ferromagnetic substance when two anisotropy constants are taken into account, and the corresponding $\Phi_{\langle 100 \rangle} = \Phi_{\langle 111 \rangle}$, $\Phi_{\langle 111 \rangle} = \Phi_{\langle 110 \rangle}$, and $\Phi_{\langle 100 \rangle} = \Phi_{\langle 110 \rangle}$ SFPT are first-order transitions. Let us note at once that the study of the first-order SFPT $\Phi_{\langle 100 \rangle} = \Phi_{\langle 110 \rangle}$ with allowance for only two magnetic-anisotropy constants is not quite correct, since in zero field the stability region for the corresponding phases about without overlapping (there do not exist the metastable-state regions that are characteristic of first-order phase transitions).¹⁾

In the investigation of SFPT in a magnetic field we neglect the critical fluctuations, which is usually fully justified in the case of spontaneous spin-reorientation transitions.^[1] The specific estimates, given in §4 of the present section, of the values of the Ginzburg numbers for typical cubic magnetic substances in the case of second-order spin-reorientation transitions in a magnetic field ($G_i \sim 10^{-5} - 10^{-4}$) justify such an approximation. Let us also note that the analysis is also valid for cubic collinear ferromagnets far from the compensation points if the magnetic-field intensity does not exceed a certain critical value that causes the appearance of a noncollinear magnetic structure.

The total number of possible (H, T) orientation phase diagrams in the (h, q) plane is equal to six, since for the three chosen H directions it is necessary to consider the cases $K_2 < 0$ and $K_2 > 0$ separately.

A. The case $H \parallel \langle 100 \rangle$, $K_2 < 0$

Minimizing (1) for $\theta_H = 0$, we easily obtain the equilibrium directions of the magnetization vector:

$$\varphi = \pi/4, \quad \theta = 0; \quad (2)$$

$$\varphi = \pi/4, \quad \cos \theta_{\perp} (3 \cos^2 \theta_{\perp} - 1) (q^{-1/2} \sin^2 \theta_{\perp}) + h = 0. \quad (3)$$

The condition (2) corresponds to the phase $\Phi_{\langle 100 \rangle}$, while the conditions (3) correspond to the field-modified (canted) phase $\Phi_{\langle 111 \rangle}$ (hereafter to be denoted by $\Phi_{\langle 111 \rangle}^c$), to which corresponds rotation of the magnetization in a (110)-type plane. Of the roots of (3) we shall be interested in only the one that goes over, as $h \rightarrow 0$, into $\theta_{\perp} = \theta_0 = \arcsin \sqrt{2/3}$.

It is not difficult to show that the stability regions for the phases $\Phi_{\langle 100 \rangle}$ and $\Phi_{\langle 111 \rangle}^c$ are determined respectively by the following conditions:

$$h + 2q \geq 0; \quad (4)$$

$$2q \cos 4\theta_{\perp} + \frac{1}{2} \sin^2 \theta_{\perp} [(2q - 3 \cos^2 \theta_{\perp} + 1) (4 \cos^2 \theta_{\perp} - 1) + \frac{1}{2} \sin^2 2\theta_{\perp}] + h \cos \theta_{\perp} \geq 0. \quad (5)$$

The first-order-SFPT line is determined from the equality of the free energies of the phases, and can be written in the form

$$\frac{1}{2} q \sin^2 2\theta_{\perp} + \frac{1}{2} (q - \cos^2 \theta_{\perp}) \sin^4 \theta_{\perp} + h (1 - \cos \theta_{\perp}) = 0. \quad (6)$$

It can be seen that as $h \rightarrow 0$ the expressions (4)–(6) go over into the conditions of Ref. 2, i.e., the $\Phi_{\langle 100 \rangle}$ phases are stable when $q \geq 0$, the $\Phi_{\langle 111 \rangle}$ phases are stable when

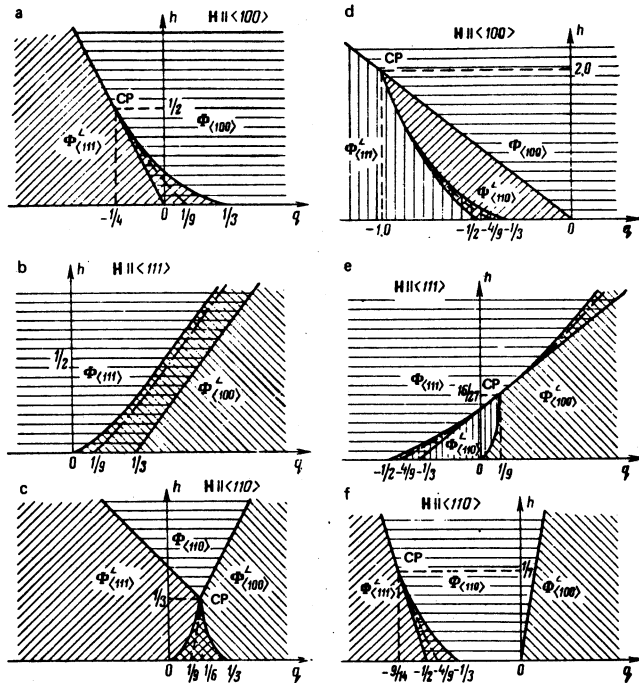


FIG. 1. Orientation phase diagrams of an unbounded cubic ferromagnet (schematic representation): a), b), and c) for $K_2 < 0$; d), e), and f) for $K_2 > 0$. The regions of phase stability are hatched; the dash-dot curves are the phase-equilibrium lines (CP—critical points; for the definitions of h and q , see (1a)).

$q \leq 1/3$, and the first-order SFPT point is determined by the condition $q = 1/9$.

An analysis shows that the stability-loss curves of the phases [the expressions (4) and (5) with the equality sign] and the phase-equilibrium curve, (6), intersect at one point on the phase diagram, after which a second-order phase transition occurs on the line $2q + h = 0$. This point is a critical point for first- and second-order transitions. To find the CP, we proceed in the following manner. The critical value of the internal parameter of the system—the angle θ —is $\theta_c = 0$. Let us expand the free energy f_0 in a series around $\theta_c = 0$:

$$f_0/K_2 = f_0^0 + \frac{1}{2} f_2 \theta^2 + \frac{1}{4} f_4 \theta^4 + \frac{1}{6} f_6 \theta^6 + \dots; \\ f_0^0 = -h, \quad f_2 = 2q + h, \quad f_4 = -\frac{1}{2} q - 1 - \frac{1}{6} h, \quad f_6 = \frac{1}{12} q + \frac{1}{2} + \frac{1}{120} h.$$

Notice that to determine the CP in the present case it is necessary to have the expansion of f_0 right up to θ^6 . As is well known, the CP is determined by the conditions $f_0 = 0, f_4 = 0, f_6 > 0$. We obtain the coordinates of the CP on the phase diagram: $q_c = -\frac{1}{4}, h_c = \frac{1}{2}$. The phase diagram for this case in the generalized coordinates (h, q) is schematically shown in Fig. 1a.

B. The Case $H \parallel \langle 111 \rangle$, $K_2 < 0$

The minimization of (1) for $\varphi_H = \pi/4$ and $\theta_H = \arcsin \sqrt{2/3}$ yields the following equilibrium directions for the crystal magnetization:

$$\varphi = \pi/4, \quad \theta = \theta_0 = \arcsin \sqrt{2/3}; \quad (7)$$

$$\varphi = \pi/4, \quad \frac{1}{2} \sin 2\theta_{\perp} \sin (\theta_{\perp} + \theta_0) (q^{-1/2} \sin^2 \theta_{\perp}) - h = 0. \quad (8)$$

The conditions (7) correspond to the $\Phi_{\langle 111 \rangle}$ phase, while the conditions (8) correspond to the $\Phi_{\langle 100 \rangle}^c$ phase (rotation of M in a (110)-type plane). Let us recall that in the expression (8) we are interested in only the root that goes over, as $h \rightarrow 0$, into $\theta_{\perp} = 0$. The stability regions for the $\Phi_{\langle 111 \rangle}$ and $\Phi_{\langle 100 \rangle}^c$ phases are determined by the conditions:

$$h - \frac{1}{2} q + \frac{1}{6} \geq 0,$$

$$2q \cos 4\theta_{\perp} + \frac{1}{2} \sin^2 \theta_{\perp} [(2q - 3 \cos^2 \theta_{\perp} + 1) (4 \cos^2 \theta_{\perp} - 1) + \frac{1}{2} \sin^2 2\theta_{\perp}] + h \cos (\theta_{\perp} - \theta_0) \geq 0, \quad (9)$$

while the phase-equilibrium curve is determined by the condition

$$\frac{1}{2} q \sin^2 2\theta_{\perp} + \frac{1}{2} (q - \cos^2 \theta_{\perp}) \sin^4 \theta_{\perp} + h [1 - \cos (\theta_{\perp} - \theta_0)] - \frac{1}{27} (9q - 1) = 0. \quad (10)$$

Analysis shows that the phase-equilibrium curve and the stability-loss curves for the phases do not intersect in the (h, q) plane, i.e., the phase-equilibrium curve always lies between the stability-loss curves. Thus, no CP exists, and the $\Phi_{\langle 111 \rangle} = \Phi_{\langle 100 \rangle}^c$ transition remains, for any value of the magnetic field, a first-order phase transition. A schematic phase diagram for this case is shown in Fig. 1b.

C. The Case $H \parallel \langle 110 \rangle$, $K_2 < 0$

A magnetic field oriented along a $\langle 110 \rangle$ -type direction ($\varphi_H = \pi/4$, $\theta_H = \pi/2$) modifies both the $\Phi_{\langle 111 \rangle}$ and the $\Phi_{\langle 100 \rangle}$ phases, which can be stable in zero field in the case when $K_2 < 0$. Let us denote them respectively by $\Phi'_{\langle 111 \rangle}$ and $\Phi'_{\langle 100 \rangle}$. Indeed, the minimization of (1) leads to the following equilibrium directions for \mathbf{M} :

$$\varphi = \pi/4, \quad \theta = \pi/2; \quad (11)$$

$$\varphi = \pi/4, \quad \sin \theta_{\perp} (q - 1/2 \sin^2 \theta_{\perp}) (3 \cos^2 \theta_{\perp} - 1) - h = 0. \quad (12)$$

The conditions (11) correspond to the $\Phi_{\langle 110 \rangle}$ phase, while the conditions (12) correspond to the phase $\Phi'_{\langle 111 \rangle}$, determined by the root that goes over, as $h \rightarrow 0$, into $\theta_{\perp} = \theta_0$. In the $\Phi'_{\langle 111 \rangle}$ phase the \mathbf{M} vector rotates in the (110) plane.

The following equilibrium directions for \mathbf{M} are also possible:

$$\theta = \pi/2, \quad \varphi = \pi/4; \quad (13)$$

$$\theta = \pi/2, \quad 2q \sin 2\varphi_{\perp} \cos(\varphi_{\perp} - \pi/4) - h = 0. \quad (14)$$

The conditions (13) correspond to the phase $\Phi_{\langle 110 \rangle}$, while the conditions (14) correspond to the phase $\Phi'_{\langle 100 \rangle}$, determined by the root that goes over into $\varphi_{\perp} = 0$ as $h \rightarrow 0$. In this phase the magnetization rotates in a (100) -type plane.

The $\Phi'_{\langle 111 \rangle} \rightleftharpoons \Phi_{\langle 110 \rangle}$ SFPT is a second-order transition on the line $h + q - 1/2 = 0$. In the region $1/6 \leq q \leq 1/3$ the stability-loss line of the $\Phi'_{\langle 111 \rangle}$ phase is determined by the expression

$$2 \sin^2 \theta_{\perp} (q - \cos^2 \theta_{\perp}) - h = 0.$$

The $\Phi'_{\langle 100 \rangle} \rightleftharpoons \Phi_{\langle 110 \rangle}$ SFPT is also a second-order transition that occurs on the line $h - 2q = 0$. In the region $0 \leq q \leq 1/6$ the stability-loss line of the $\Phi_{\langle 100 \rangle}$ phase is determined by the equation

$$2q - (q + 1/2) \sin^2 2\varphi_{\perp} + h \cos(\varphi_{\perp} - \pi/4) = 0.$$

Since the regions of stability of the angular phases $\Phi'_{\langle 111 \rangle}$ and $\Phi'_{\langle 100 \rangle}$ overlap, the $\Phi'_{\langle 111 \rangle} \rightleftharpoons \Phi'_{\langle 100 \rangle}$ SFPT is a first-order transition. The equilibrium curve of these phases is determined by the system of equations (12), (14), and the equation that follows from the equality of the free energies of the angular phases:

$$\begin{aligned} 1/4 q \sin^2 2\theta_{\perp} + 1/4 (q - \cos^2 \theta_{\perp}) \sin^4 \theta_{\perp} - h \sin \theta_{\perp} \\ = 1/4 q \sin^2 2\varphi_{\perp} - h \cos(\varphi_{\perp} - \pi/4). \end{aligned}$$

Notice that the second-order phase transitions $\Phi'_{\langle 111 \rangle} \rightleftharpoons \Phi_{\langle 110 \rangle}$ and $\Phi'_{\langle 100 \rangle} \rightleftharpoons \Phi_{\langle 110 \rangle}$ do not possess critical points, but the lines of these transitions intersect the equilibrium curve of the angular phases at the CP ($q_c = 1/6$, $h_c = 1/3$) of the first-order phase transition $\Phi'_{\langle 111 \rangle} \rightleftharpoons \Phi'_{\langle 100 \rangle}$.

As was to be expected, for $h \rightarrow 0$ the phase $\Phi_{\langle 110 \rangle}$ is not stable in zero field. The phase diagram is shown in Fig. 1c.

D. The Case $H \parallel \langle 100 \rangle$, $K_2 > 0$

If $K_2 > 0$, then according to Ref. 2, the $\Phi_{\langle 111 \rangle}$ phases are stable in zero field when $q \leq -1/3$, the $\Phi_{\langle 110 \rangle}$ phases when $-1/2 \leq q \leq 0$, and the $\Phi_{\langle 100 \rangle}$ phases when $q \geq 0$, while the $\Phi_{\langle 111 \rangle} \rightleftharpoons \Phi_{\langle 110 \rangle}$ and $\Phi_{\langle 110 \rangle} \rightleftharpoons \Phi_{\langle 100 \rangle}$ SFPT points are determined respectively by the conditions $q = -4/9$ and $q = 0$. Therefore, for any of the three considered orientations of the field three phases should be present on the phase diagrams.

The application of a magnetic field along a $\langle 100 \rangle$ -type axis modifies the phases $\Phi_{\langle 111 \rangle}$ and $\Phi_{\langle 110 \rangle}$. As a result of the minimization of (1), we obtain the following \mathbf{M} orientation:

$$\varphi = \pi/4, \quad \theta = 0; \quad (15)$$

$$\varphi = \pi/4, \quad \cos \theta_{1\perp} (3 \cos^2 \theta_{1\perp} - 1) (q + 1/2 \sin^2 \theta_{1\perp}) + h = 0. \quad (16)$$

The conditions (15) determine the phase $\Phi_{\langle 100 \rangle}$, while (16) determines the phase $\Phi'_{\langle 111 \rangle}$ (\mathbf{M} lies in a (110) -type plane), the root that goes over into $\theta_{1\perp} = \theta_0$ as $h \rightarrow 0$ being of interest to us.

The following equilibrium directions for \mathbf{M} are also possible:

$$\varphi = 0, \quad \theta = 0; \quad (17)$$

$$\varphi = 0, \quad 2q \cos \theta_{2\perp} \cos 2\theta_{2\perp} + h = 0. \quad (18)$$

The conditions (17) correspond to the phase $\Phi_{\langle 100 \rangle}$, while (18) correspond to the phase $\Phi'_{\langle 110 \rangle}$, determined by the root that goes over, as $h \rightarrow 0$, into $\theta_{2\perp} = \pi/4$ (\mathbf{M} lies in a (100) -type plane).

It is easy to show that the transitions between the angular phases and the collinear phase are second-order SFPT that occur on the straight line $2q + h = 0$.

The regions of stability of the phases $\Phi'_{\langle 111 \rangle}$ and $\Phi'_{\langle 110 \rangle}$ are bounded by this straight line (Fig. 1d), as well as by the curves defined respectively by the equations $q + \cos^2 \theta_{1\perp} = 0$ and $2q \cos 4\theta_{2\perp} + h \cos \theta_{2\perp} = 0$.

The regions of stability of the angular phases overlap, and the $\Phi'_{\langle 111 \rangle} \rightleftharpoons \Phi'_{\langle 110 \rangle}$ SFPT is a first-order transition. The phase-equilibrium curve is determined by the system of equations (16), (18), (19):

$$1/4 q \sin^2 2\theta_{1\perp} + 1/4 (q + \cos^2 \theta_{1\perp}) \sin^4 \theta_{1\perp} - h \cos \theta_{1\perp} = 1/4 q \sin^2 2\theta_{2\perp} - h \cos \theta_{2\perp}. \quad (19)$$

As in the preceding case, for $h > 0$ the second-order phase transitions between the angular phases and the collinear phase do not possess critical points; the lines of these transitions intersect the equilibrium curve of the angular phases at the CP ($q_c = -1$, $h_c = 2$) of the first-order SFPT $\Phi'_{\langle 111 \rangle} \rightleftharpoons \Phi'_{\langle 110 \rangle}$.

E. The Case $H \parallel \langle 111 \rangle$, $K_2 > 0$

In this case the magnetic field cants the phases $\Phi_{\langle 100 \rangle}$ and $\Phi_{\langle 110 \rangle}$. The minimization of the free energy (1) leads to the following equilibrium directions for the magnetization:

$$\varphi = \pi/4, \quad \theta = 0; \quad (20)$$

$$\varphi = \pi/4, \quad \frac{1}{2} \sin 2\theta_{\perp} \sin(\theta_{\perp} + \theta_0) (q + \frac{1}{2} \sin^2 \theta_{\perp}) - h = 0. \quad (21)$$

The conditions (20) determine the phase $\Phi_{(111)}$, while Eq. (21) determines the angular phases $\Phi_{(100)}^{\prime}$ and $\Phi_{(110)}^{\prime}$. It should be noted that to the phase $\Phi_{(100)}^{\prime}$ corresponds the root that goes over into $\theta_{1\zeta} = 0$ as $h \rightarrow 0$, while to the phase $\Phi_{(110)}^{\prime}$ corresponds the root that goes over into $\theta_{2\zeta} = \pi/2$ [in both phases \mathbf{M} rotates in a (110)-type plane].

The region of stability of the phase $\Phi_{(111)}$ is determined by the condition

$$h - \frac{1}{2} q - \frac{1}{2} h \geq 0.$$

In the interval $0 \leq q \leq 1/9$ the equation of the stability-loss line of the phase $\Phi_{(100)}^{\prime}$ has the form

$$\sin \theta_{1\zeta} [-\sqrt{6} \sin^2 \theta_{1\zeta} (q + \cos^2 \theta_{1\zeta}) + h] = 0, \quad (22)$$

while in the range $q > 1/9$

$$2q \cos 4\theta_{1\zeta} + \frac{1}{2} \sin^2 \theta_{1\zeta} [(2q + 3 \cos^2 \theta_{1\zeta} - 1) (4 \cos^2 \theta_{1\zeta} - 1) - \frac{1}{2} \sin^2 2\theta_{1\zeta}] + h \cos(\theta_{1\zeta} - \theta_0) = 0. \quad (23)$$

For the phase $\Phi_{(110)}^{\prime}$, the stability lines in the intervals $0 \leq q \leq 1/9$ and $-\frac{1}{2} \leq q \leq 0$ are also described respectively by Eqs. (22) and (23), with the only difference that the root $\theta_{2\zeta}$ of Eq. (21) should be used.

In the case under consideration the SFPT between the collinear and the angular phases are first-order transitions, and the phase-equilibrium lines are determined by the equation

$$\frac{1}{2} q \sin^2 2\theta_{1,2\zeta} + \frac{1}{2} (q + \cos^2 \theta_{1,2\zeta}) \sin^4 \theta_{1,2\zeta} + h [1 - \cos(\theta_{1,2\zeta} - \theta_0)] - \frac{1}{2} q - \frac{1}{2} h = 0. \quad (24)$$

The transition $\Phi_{(100)}^{\prime} \rightleftharpoons \Phi_{(110)}^{\prime}$ is also a first-order SFPT. The distinctive feature of the transition, which consists in the coincidence of the phase-equilibrium with the stability-loss lines, is, as has already been noted, due to a certain incorrectness in the study of this transition in the model with two anisotropy constants.

As can be seen from Fig. 1e, the phase-equilibrium lines of all the three first-order transitions terminate at one first-order SFPT critical point. Proceeding in the same way as in the case A, i.e., expanding f_0 around the critical value of the internal parameter of the system, $\theta_c = \theta_0$, we obtain

$$f_0/K_2 = f_0^0 + \frac{1}{2} f_2 \psi^2 + \frac{1}{2} f_3 \psi^3 + \frac{1}{2} f_4 \psi^4 + \dots,$$

where

$$f_0^0 = \frac{1}{2} q + \frac{1}{2} h, \quad f_2 = -\frac{1}{2} q - \frac{1}{2} h, \quad f_3 = \sqrt{2} q - \sqrt{2} h, \\ f_4 = \frac{1}{2} q + \frac{1}{2} h, \quad \psi = \theta - \theta_0.$$

For any such expansion (the presence of the term $\sim \psi^3$) the critical point is an isolated second-order transition point, and can be found from the condition $f_2 = 0$, $f_3 = 0$, and $f_4 \geq 0$. Its coordinates are: $q_c = 1/9$, $h_c = 16/27$.

F. The Case $H \parallel (110)$, $K_2 > 0$

The minimization of (1) leads to the following equilib-

rium orientations for \mathbf{M} :

$$\varphi = \pi/4, \quad \theta = \pi/2; \quad (25)$$

$$\varphi = \pi/4, \quad \sin \theta_{\perp} (q + \frac{1}{2} \sin^2 \theta_{\perp}) (3 \cos^2 \theta_{\perp} - 1) - h = 0. \quad (26)$$

The conditions (25) correspond to the phase $\Phi_{(110)}$, while the conditions (26) correspond to the field-modified phase $\Phi_{(111)}$. Notice that we are interested in that root of Eq. (26) which goes over into $\theta_{\perp} = \theta_0$ as $h \rightarrow 0$. It is also possible for \mathbf{M} to have the equilibrium directions determined by the conditions (14), which correspond to the phase $\Phi_{(100)}^{\prime}$.

The $\Phi_{(100)}^{\prime} \rightleftharpoons \Phi_{(110)}^{\prime}$ SFPT is a second-order transition that occurs on the line $h - 2q = 0$ (the transition line and the stability-loss lines of the phases coincide; see Fig. 1f).

For $q < -\frac{1}{2}$ the phase $\Phi_{(110)}$ loses its stability on the line $h + q + \frac{1}{2} = 0$. The stability-loss line for the $\Phi_{(111)}$ phase in the interval $-9/14 < q < -1/3$ is determined by the expression

$$2q \cos 4\theta_{\perp} + \frac{1}{2} \sin^2 \theta_{\perp} [(2q + 3 \cos^2 \theta_{\perp} - 1) (4 \cos^2 \theta_{\perp} - 1) - \frac{1}{2} \sin^2 2\theta_{\perp}] + h \sin \theta_{\perp} = 0. \quad (27)$$

The $\Phi_{(110)}^{\prime} \rightleftharpoons \Phi_{(111)}^{\prime}$ SFPT is a first-order transition, the transition line being expressible in the form

$$\frac{1}{2} q \sin^2 2\theta_{\perp} + \frac{1}{2} (q + \cos^2 \theta_{\perp}) \sin^4 \theta_{\perp} - h \sin \theta_{\perp} - \frac{1}{2} q + h = 0. \quad (28)$$

In the present case a CP also exists. The coefficients of the free-energy expansion around the critical value of the parameter of the system, $\theta_c = \pi/2$, have the form

$$f_0^0 = \frac{1}{2} q - h, \quad f_2 = q + \frac{1}{2} h, \quad f_3 = -\frac{1}{2} q - \frac{1}{2} h, \\ f_4 = \frac{1}{2} q + \frac{1}{2} h.$$

The CP is determined by the same conditions as in the case A. Its coordinates are:

$$q_c = -\frac{1}{4}, \quad h_c = \frac{1}{4}. \quad (29)$$

In fields stronger than h_c , the $\Phi_{(110)} \rightleftharpoons \Phi_{(111)}$ SFPT is a second-order transition on the line $h + q + \frac{1}{2} = 0$. Consequently, the point with the coordinates (29) is a CP for first- and second-order transitions.

Notice that in the cases B-F the conditions for the stability of the phases $\Phi_{(100)}$, $\Phi_{(111)}$, and $\Phi_{(110)}$ in zero field, as well as the SFPT points agree with the data of Ref. 2.

§2. Magnetization Curves of Cubic Ferromagnets

The equations determining the equilibrium directions of the magnetization allow us to compute the magnetization curves of cubic ferromagnetic substances. These curves are shown in Fig. 2 for some typical values of the parameter q . The kinks that appear on their reaching saturation correspond to second-order SFPT points. First-order SFPT on the magnetization curves arise in two ways. If we neglect the hysteresis phenomena, i.e., assume that metastable states are not realized, and that the condition for a transition is the equality of the

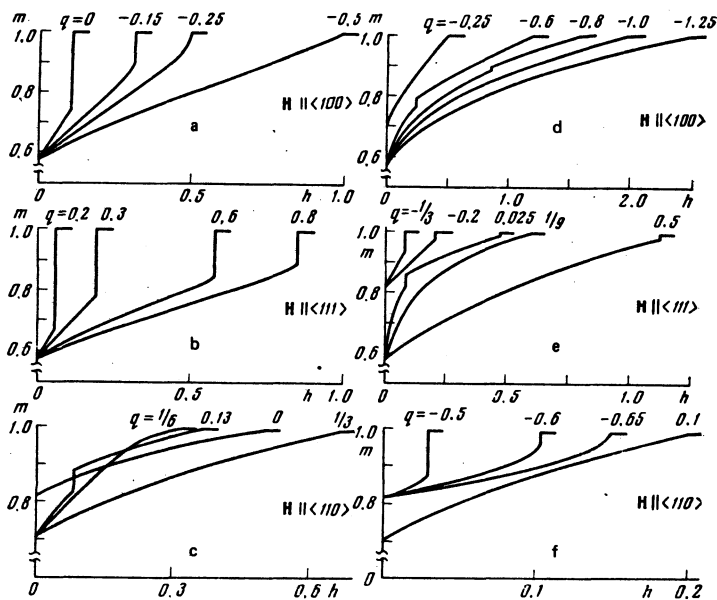


FIG. 2. Theoretical magnetization curves of an unbounded cubic ferromagnet without allowance for the metastable states that arise in first-order SFPT ($m = M_h/M_0$): a), b), and c) for $K_2 < 0$; d), e), and f) for $K_2 > 0$. The curves have been constructed for typical values of the parameter q .

free energies of the phases, then the magnetization jumps culminating in the attainment of the state of saturation correspond to first-order transitions from angular into collinear phases. Certain curves of this kind are discussed in, for example, Ref. 12. To a first-order transition between angular phases also corresponds a jump in the magnetization, but after the jump the magnetization continues to grow because of the noncompletion of the rotation process. The possibility of such transitions is pointed out in Ref. 20. And, finally, in the case E (see §1) there can, in principle, occur two magnetization jumps in the interval $0 < q < 1/9$ (see Fig. 2e).

§3. The Domain (Interphase) Boundaries Associated with First-Order SFPT

In §1 we considered the uniform distribution of magnetization in a cubic magnetic substance of infinite dimensions. The case is somewhat different in crystals of finite size, in which owing to the magnetic dipole interaction the so-called intermediate state (which is one in which the domains of the phases that are possible for the first-order SFPT in question are arranged in turn) turns out to be energetically advantageous. In all the above-considered cases, a transition from one phase into another is caused by a change in the external magnetic field (or temperature). It is known that one of the conditions for the coexistence of the various phases near a first-order phase transition point is the constancy of the internal magnetic field in the crystal,^[18] this constancy being secured when the external magnetic field H_0 changes by a redistribution of the parts of the material in each of the phases.

The nature of the domain boundaries (DB) arising in a first-order SFPT in the absence of a magnetic field was studied in the work published in Ref. 2. We shall dwell on the investigation of DB in cubic magnetic substances in external magnetic fields. Of special interest is the investigation in question near the first-order SFPT

critical points considered in Subsecs. A, E, and F of §1.

To study the magnetization distribution at a DB, which can be regarded as an inhomogeneity, we should add to the free energy (1) terms that arise from these inhomogeneities and have, in the main, an exchange character:

$$f_{inh} = 1/2 \alpha' (\partial M / \partial x_i)^2,$$

where α' is the constant of the inhomogeneous exchange interaction. Below we shall study those DB at which the rotation of the vector M occurs in (110)-type planes.

A. The First-Order SFPT $\Phi_{(100)} \rightleftharpoons \Phi_{(111)}$ ($K_2 < 0$)

In this case, near the CP, the free energy can be written in the form

$$f_{tot} = 1/2 \alpha (\theta')^2 + f_0 \theta + 1/2 f_2 \theta^2 + 1/4 f_4 \theta^4 + 1/6 f_6 \theta^6 + \dots \quad (30)$$

Here $\theta' = d\theta/d\eta$, where η is the coordinate in the direction perpendicular to the DB plane. By varying the expression (30), we can obtain an equation for the distribution of the magnetization at the DB:

$$\theta'' + \alpha^{-1} \theta (f_2 + f_4 \theta^2 + f_6 \theta^4) = 0.$$

Its first integral has the form

$$(\theta')^2 - 2\alpha^{-1} \theta^2 (1/2 f_2 + 1/4 f_4 \theta^2 + 1/6 f_6 \theta^4) = \text{const.}$$

We find the constant of the integration either from the condition $\theta(\eta)|_{\eta \rightarrow +\infty} = 0, \theta'(\eta)|_{\eta \rightarrow +\infty} = 0$ (this implies that the homogeneous phase $\Phi_{(100)}$ occurs to the right of the DB), or from the condition $\theta(\eta)|_{\eta \rightarrow -\infty} = \theta_0, \theta'(\eta)|_{\eta \rightarrow -\infty} = 0$ (to the left of the DB is the homogeneous phase $\Phi_{(111)}$). It is not difficult to verify that the two values for the constant of integration coincide. This is connected with the fact that the domains of the indicated phase are in thermodynamic equilibrium, i.e., the expression (30) for $\eta \rightarrow \pm\infty$ is analyzed on the phase-equilibrium curve

(8), the equation for which has, near the CP, the form

$$1/2f_2 + 1/2f_1\theta^2 + 1/2f_0\theta^4 = 0.$$

Thus, we can write

$$(\theta')^2 - 2\alpha^{-1}\theta^2(1/2f_2 + 1/2f_1\theta^2 + 1/2f_0\theta^4) = 0. \quad (31)$$

Integrating Eq. (31), we obtain

$$\theta = \theta_{\perp} (3e^{\eta/\eta_0} + 1)^{-1/2}, \quad \theta_{\perp}^2 = -4f_2/f_1, \quad \eta_0 = 1/2(\alpha/f_2)^{1/2}. \quad (32)$$

Notice that the indicated expression for θ_{\perp}^2 is valid only on the phase-equilibrium curve. The quantity η_0 has the meaning of an effective DB thickness, and, as can be seen from the expression (32), the effective DB thickness increases as the CP is approached along the phase-equilibrium curve.

Knowledge of the magnetization distribution at the DB allows the computation of the surface magnetization value:

$$\sigma = \frac{1}{S} \int_{-\infty}^{+\infty} d\eta (f_{101} - f_0),$$

which yields

$$\sigma = -1/2\alpha^{1/2}f_2^{1/2}f_1/f_0.$$

It can be seen that the surface-energy density of the DB tends to zero as the CP is approached. This is connected with the fact that the difference between the phases disappears at the CP.

B. The First-Order SFPT $\Phi_{(111)} \leftrightarrow \Phi_{(110)}$ ($K_2 > 0$)

Arguments and computations similar to the foregoing lead to the following magnetization distribution at the DB for this case:

$$\psi = \psi_{\perp} (e^{\eta/\eta_0} + 1)^{-1}, \quad \psi_{\perp} = -3f_2/f_1, \quad \psi = \theta - \theta_0, \quad \eta_0 = (\alpha/f_2)^{1/2}.$$

The surface-energy density of the DB near the CP is given in this case by

$$\sigma = 1/2\alpha^{1/2}f_2^{1/2}f_1^2/f_0^2.$$

C. The First-Order SFPT $\Phi_{(110)} \leftrightarrow \Phi'_{(111)}$ ($K_2 > 00$)

It can be shown that in this case

$$\psi = \psi_{\perp} (3e^{\eta/\eta_0} + 1)^{-1/2}, \quad \psi_{\perp}^2 = -4f_2/f_1, \quad \psi = \theta - \pi/2, \quad \eta_0 = 1/2(\alpha/f_2)^{1/2};$$

$$\sigma = -1/2\alpha^{1/2}f_2^{1/2}f_1/f_0.$$

§4. The Region of Applicability of the Landau Theory

Let us estimate the region of applicability of the Landau theory as applied to the description of second-order SFPT in cubic ferromagnets. It is not difficult to show

that the value of the Ginzburg number^[21] in the case of interest to us can be estimated from the following formula:

$$G_i = \frac{C|K_2|(q - q_c)^2 k^2 T_i}{A^2 \partial q / \partial T}. \quad (33)$$

Here T_i is the transition temperature, A is the exchange-coupling constant, k is the Boltzmann constant, C is a constant of the order of unity, that depends on the type of second-order SFPT. Let us carry out the estimate for the ferrite-garnets $Tb_xY_{3-x}Fe_5O_{12}$ and $Sm_3Fe_5O_{12}$, which have been experimentally investigated by us (see below in Sec. II), these ferrite-garnets being typical cubic ferrimagnets with moderate ($\sim 10^4$ erg/cm³) and substantial ($\sim 10^6$ erg/cm³) anisotropy constants. Using the $Tb_{0.1}Y_{2.9}Fe_5O_{12}$ (the transition $\Phi'_{(111)} \leftrightarrow \Phi_{(100)}$) the values $C=2$, $q_c = -1/4$, $A \approx 4.4 \times 10^{-7}$ erg/deg, as well as the values $q \approx -0.61$, $\partial q / \partial T \approx 0.04$ deg⁻¹, $K_2 = -1.3 \times 10^4$ erg/cm³, which correspond to $T_i = 135$ K,^[5] we can obtain that $G_i \approx 1.5 \times 10^{-5}$. Similarly, for $Sm_3Fe_5O_{12}$ (the transition $\Phi'_{(111)} \leftrightarrow \Phi_{(110)}$), $C=7/2$, $q_c = -9/14$; the values $q = -0.78$, $\partial q / \partial T \approx 0.03$ deg⁻¹, and $K_2 = 1.8 \times 10^6$ erg/cm³ for $T_i = 78$ K,^[6] we find that $G_i \approx 2 \times 10^{-4}$. Since the criterion for the applicability of the Landau theory^[21] is the condition

$$\tau = \left| \frac{T - T_i}{T_i} \right| \gg G_i,$$

we can conclude that for the purpose of describing SFPT in cubic magnets the theory is inapplicable only in a very narrow interval of relative temperatures ($\tau \sim 10^{-3}$) near T_i .

II. EXPERIMENTAL STUDY OF SFPT IN THE IRON GARNETS

§1. Samples and Measurement Procedure

Investigations of the effect of an external magnetic field on SFPT were carried out on the single crystals of the iron garnets of the system $Tb_xY_{3-x}Fe_5O_{12}$ and the single crystals of the iron garnet $Sm_3Fe_5O_{12}$ that were used by us earlier for the study of reorientation in zero field.^[5,6] The technology for growing single crystals is described in Refs. 6 and 22. Spherical samples of diameter 1–4 mm or samples in the form of thin disks were used.

The magnetic anisotropy constants were measured by the torque method in fields of up to 14 kOe. The temperature dependences of the constants K_1 and K_2 of ferrites of the system $Tb_xY_{3-x}Fe_5O_{12}$ have been measured by Borodin *et al.*^[6] and Kolacheva *et al.*^[23] Additional measurements have also been made of the constants for terbium-yttrium garnets in the low-temperature region 10–77 K and for the samarium garnet in the 50–60-K range.

The curves of magnetization of the single crystals along the various directions were measured with the aid of a vibrating magnetometer in fields of up to 10 kOe.

The orientation of the samples was effected by a magnetic method.

The ^{57}Fe -NMR spectra were measured, using the Hahn two-pulse spin-echo technique, on a spectrometer with facilities for frequency sweep and automatic spectrum recording. The necessary resolving power was secured by the choice of exciting pulses of substantial width (5–10 μsec); to raise the sensitivity we used a stroboscopic integrator.

The components of the differential susceptibility were measured in the following manner. In the magnet gap was placed a device consisting of two pairs of coils arranged in such a way that the axis of one pair was parallel, and that of the other perpendicular, to the constant field H_0 . A spherical sample was placed at the point of intersection of the coil axes. To measure χ_{\perp} , the coils of parallel orientation were fed by an audio-frequency oscillator ($F=20$ kHz), and a signal, proportional to χ_{\perp} , was tapped from the coils of perpendicular orientation. An electrical compensation of the emf's resulting from the inevitable errors in the relative orientation of the coils was carried out. The component χ_{\parallel} was measured by the bridge method at the same frequency, using only the coils of parallel orientation. All the χ measurements were relative.

§2. Results of the Experiment and their Discussion

In Fig. 3a we present, for the case of external magnetic fields directed along a $\langle 111 \rangle$ -type axis, magnetization curves of the iron garnet $\text{Tb}_{0.1}\text{Y}_{2.9}\text{Fe}_5\text{O}_{12}$, measured on a spherical sample in the temperature range 10–106 K. In this range the parameter q varies from a value of 0.1 to a value of 0.39 ($K_2 < 0$), and, in accordance with the diagram shown in Fig. 1b, the easy axes are the $\langle 100 \rangle$ -type directions (a result which is confirmed by the experimental data of Ref. 5) and the first-order SFPT $\Phi'_{\langle 100 \rangle} \rightleftharpoons \Phi'_{\langle 111 \rangle}$ should occur in a magnetic field $H_0 \parallel \langle 111 \rangle$.

Indeed, the magnetization curves exhibit pronounced anomalies, which confirm the existence of this transi-

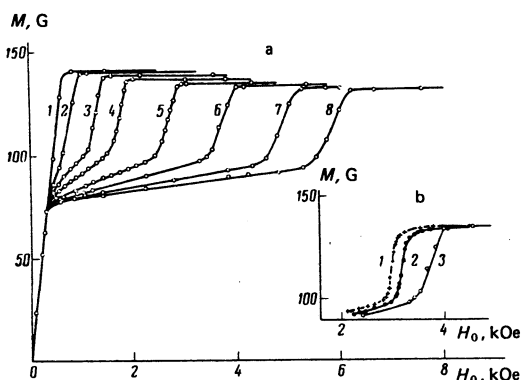


FIG. 3. Curves of magnetization of the iron garnet $\text{Tb}_{0.1}\text{Y}_{2.9}\text{Fe}_5\text{O}_{12}$ along the $\langle 111 \rangle$ axis, measured in an increasing magnetic field. a) Spherical sample at T K: 1) 106.0, 2) 77.3, 3) 58.5, 4) 48.8, 5) 37.4, 6) 29.8, 7) 21.0, 8) 10.0. b) $T = 29.8$ K: 1) disk with $t/d \approx 0.05$; 2) disk with $t/d = 0.14$; 3) sphere.

tion. Notice that the difference between the observed anomalies and the way the magnetization should behave in an unbounded crystal consists in the following. First, in the region of an anomaly the dependence $M(H_0)$ has a slope close to the slope of the initial section of the magnetization curve, where the magnetization is accomplished through the shifting of the DB and the internal field is virtually equal to zero. Secondly, the hysteresis of the magnetization curves in the region of the anomalies is small, in any case, it is more than an order of magnitude smaller than the hysteresis given by the theory in the homogeneous case (we have in mind the width—in field terms—of the overall metastable-phase region).

These differences find a natural explanation if it is assumed that an intermediate state is realized in the sample during the first-order phase transition under investigation, i.e., the sample separates into domains of the phases $\Phi'_{\langle 100 \rangle}$ and $\Phi'_{\langle 111 \rangle}$, which coexist in some field range. This range can be roughly estimated to be $\Delta H_0 \approx N\Delta M$, where N is the demagnetization factor of the sample and ΔM is the magnitude of the magnetization jump. The last condition corresponds to the constancy of the internal field in a sample of finite size during the first-order phase transition. Check measurements performed on samples with different demagnetization factors qualitatively confirm this result.

In Fig. 3b we present three plots of $M(H_0)$ in the region of the anomalies for a spherical sample and disks with different values of the ratio t/d . The increase of the slope of the dependence $M(H_0)$ as the demagnetization factor decreases is clearly visible. The presence of a transitional state and, consequently, of a TDS allows a qualitative explanation of the small width—in field terms—of the hysteresis loop. Analysis of the phase portrait of the equation describing the magnetization distribution at a DB for a fixed $q(T)$ value that allows the occurrence of the first-order transition and for different magnetic-field values shows that the angular and collinear phases coexist only in a narrow range of internal fields near the phase-equilibrium curve and that the new phase develops continuously and reversibly from “nuclei” that are the walls between the domains of the old phase. The virtual absence of hysteresis in the case of the investigation of the first-order SFPT in these same compounds with respect to temperature has been explained in much the same way.^[2,5,6] The computations in Sec. I, §3 confirm the coexistence of the phases on the phase-equilibrium curve near the CP of the first-order transition. It is interesting that the observation of this same transition in pulsed magnetic fields allows the detection of substantial hysteresis (see the low-field transition in Fig. 1 of Ref. 24). It is possible that, in the case of a high rate of change of the field, the TDS does not have time to develop, and the behavior of the reorientation is the same as in the homogeneous case. But this surmise requires additional verification.

In Fig. 4 we have plotted on the theoretical phase diagram for the phase transitions $\Phi'_{\langle 100 \rangle} \rightleftharpoons \Phi'_{\langle 111 \rangle}$ experimental points obtained from the above-presented magnetiza-

tion curves of the iron garnet with $x=0.1$, as well as from those of the ferrite with $x=0.26$, whose magnetization curves have an entirely similar shape. The solid lines represent the stability-loss curves of the phases, while the dash-dot line represents the phase-equilibrium curve, which was computed numerically from the formulas (8)–(10). In processing the experimental data we took the degaussing field into account, so that along the ordinate axis we have plotted the parameter h for an internal-field value given by $H = H_{0z} - (4\pi/3)M_z$, where H_{0z} and M_z are respectively the external field and the magnetization corresponding to the midpoint of the "anomalous" section of the $M(H_0)$ curve. In the same figure we have plotted a point for a disk with $t/d \approx 0.05$, when it can be assumed that $H \approx H_0$. It can be seen that the experimental data for the two ferrites of different compositions lie near the phase-equilibrium curve of the generalized phase diagram. This also corroborates the conclusion that the intermediate state associated with first-order phase transitions in cubic ferromagnets is realized near the equilibrium curve for the phases.

The coexistence of the phases $\Phi_{\langle 100 \rangle}^c$ and $\Phi_{\langle 111 \rangle}$ during first-order phase transitions in single crystals with $x=0.1$ has been demonstrated by ^{57}Fe -NMR method at $T=4.2$ K. The NMR spectra of the octahedral ions Fe^{3+} in a spherical sample ($d=3.9$ mm) were measured in the geometry: $H_0 \parallel \langle 111 \rangle, H_{\text{ext}} \perp H_0$. These spectra, which were measured as the magnetic field was decreased, are shown in Fig. 5. We shall not discuss the theory, developed in Refs. 25 and 26 and summarized in Ref. 5 from the standpoint of the possibility of investigating magnetic structures, of ^{57}Fe -NMR spectra of the iron garnets. It follows from Fig. 1 of Ref. 5, which depicts the angular dependence of the three branches of the spectrum of the octahedral ions as \mathbf{M} is rotated in the (110) plane, that for the $\Phi_{\langle 100 \rangle}^c$ phases we should observe a single line (denoted by a) that, when \mathbf{M} deviates from a $\langle 100 \rangle$ -type axis (i.e., in the case of the angular phases $\Phi_{\langle 100 \rangle}^c$) should split up into three lines with intensity ratios of 1:2:1. On the other hand, the spectrum of the collinear phase $\Phi_{\langle 111 \rangle}$ should consist of two lines a^I and a^{II} with an intensity ratio of 1:3. Taking these observations and the fact that the spectra recorded as the field was decreased and those recorded in increasing field have identical shape into account, we can interpret the spectra shown in Fig. 5 in the following manner. In

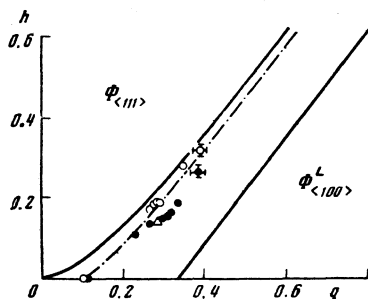


FIG. 4. Theoretical phase diagram for $H_0 \parallel \langle 111 \rangle$ ($K_2 < 0$) together with experimental data for iron garnets of the system $\text{Tb}_x \text{Y}_{2-x} \text{Fe}_5 \text{O}_{12}$: \bullet) $x=0.1$, sphere; Δ) $x=0.1$, disk with $t/d \approx 0.05$; \circ) $x=0.26$, sphere. Temperature range: 10–77 K. The mean error values are indicated (see explanations in text).

zero field the spectrum consists of a single line, a , i.e., only the $\Phi_{\langle 100 \rangle}$ phases are realized. As the intensity of the external field increases, the line a indeed splits up into three lines with intensity ratios close to the theoretical values (this group of lines is designated in Fig. 5 as a^c), i.e., the angular phases $\Phi_{\langle 100 \rangle}^c$ are realized. Starting from some value of the field, there appear in the spectrum lines, a^I and a^{II} , corresponding to the $\Phi_{\langle 111 \rangle}$ phases, and, what is more, an increase in the field does not affect the magnitude of the splitting of the lines in the group a^c , but only causes a redistribution of the intensities of the lines of the $\Phi_{\langle 100 \rangle}^c$ and $\Phi_{\langle 111 \rangle}$ phases right down to the total disappearance of the a^c lines. The spectra in this field range unambiguously prove the coexistence of the collinear phase and the angular phases, i.e., the existence of the intermediate state. As the field intensity H_0 increases further, only the lines a^I and a^{II} , which characterize the phase $\Phi_{\langle 111 \rangle}$, remain in the spectrum.

We have compared the maximum angle of deviation of the magnetization \mathbf{M} from a $\langle 100 \rangle$ -type axis, determined from the NMR spectra, i.e., the angle θ_z of the $\Phi_{\langle 100 \rangle}^c$ phase in the intermediate state, with its theoretical value on the phase-equilibrium curve. On the basis of the distance between the lines a^I and a^{II} (1.05 MHz) and the splitting of the lines in the group a^c (0.28 MHz), we can, using the theoretical angular dependence of the NMR frequencies,^[5] easily find that $\theta_z = 7.2^\circ$. Extrapolation to $T=4.2$ K yields a value for the parameter q within the limits 0.2–0.22. On the phase-equilibrium curve (10) to such values correspond theoretical values for θ_z , (8), in the range 9.6 – 11° . Allowing for a possible error in the determination of q as a result of the extrapolation

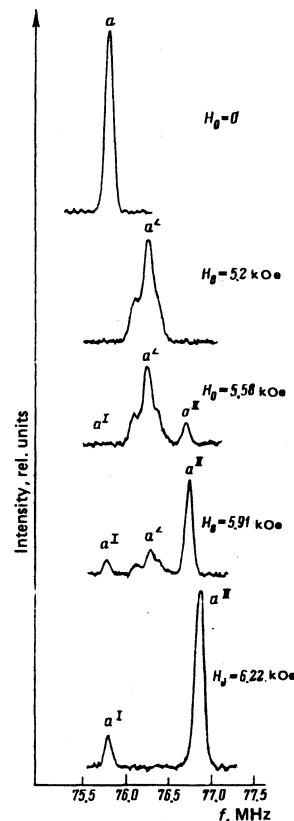


FIG. 5. ^{57}Fe -NMR spectra for the octahedral Fe^{3+} ions of the iron garnet $\text{Tb}_{0.1} \text{Y}_{2.9} \text{Fe}_5 \text{O}_{12}$ ($T=4.2$ K), measured in a decreasing field. The symbols are explained in the text.

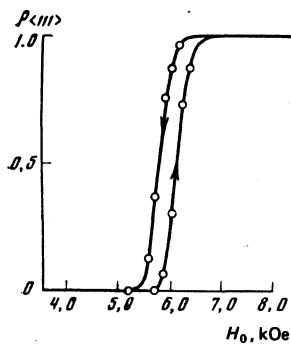


FIG. 6. Dependence of the relative volume of the $\Phi_{\langle 111 \rangle}$ phases of a monocrystalline sphere of the iron garnet $\text{Tb}_{0.1}\text{Y}_{2.9}\text{Fe}_5\text{O}_{12}$ on the external magnetic field intensity for $T = 4.2$ K and $H_0 \parallel \langle 111 \rangle$.

from 10 to 4.2 K and for the resolution of the NMR spectra, we can acknowledge the agreement between the obtained values to be quite satisfactory. Thus, the NMR method also corroborates the inference of the existence of a transitional state near the phase-equilibrium curve. Notice also that the direct observation of the coexistence of the domains of the $\Phi_{\langle 100 \rangle}$ and $\Phi_{\langle 111 \rangle}$ phases has been accomplished by Belyaeva *et al.*^[14] with the aid of magneto-optical methods in the case of magnetization along a $\langle 111 \rangle$ -type axis ($T = 4.2$ K) of a thin erbium-iron-garnet ($\text{Er}_3\text{Fe}_5\text{O}_{12}$) plate. In this cubic ferromagnet, as in the terbium yttrium iron garnets, the easy axes at $T = 4.2$ K are the $\langle 100 \rangle$ directions.

The NMR technique allows us to reproduce the field dependences of the volumes of the coexisting phases in the intermediate state. In Fig. 6 we show the dependence of the relative volume of the $\Phi_{\langle 111 \rangle}$ phases, $\rho_{\langle 111 \rangle} = v_{\langle 111 \rangle} / (v_{\langle 111 \rangle} + v'_{\langle 100 \rangle})$, which is identified with the field dependence of the ratio, $[I(a^I) + I(a^{II})] / [I(a^I) + I(a^{II}) + I(a^C)]$, of the intensities of the lines. The measurements were performed both in increasing, and in decreasing, field. It can be seen that the width of the hysteresis loop is quite small (about 300 Oe). The main cause of the hysteresis phenomena in the transitional state is, in our opinion, the retardation of the domain boundaries by the defects during the reconstruction of the TDS. Some experimental data given below are in accord with such a conjecture.

The investigated $\Phi'_{\langle 100 \rangle} \rightleftharpoons \Phi_{\langle 111 \rangle}$ transition is the most suitable transition for a quantitative comparison of the theory with experiment, since the maximum magnitude of the magnetization jump is quite substantial (up to $0.42M_0$) and the region of metastable states is wide. The maximum magnetization jumps expected in the investigation of the first-order SFPT $\Phi'_{\langle 110 \rangle} \rightleftharpoons \Phi_{\langle 111 \rangle}$ and $\Phi'_{\langle 111 \rangle} \rightleftharpoons \Phi_{\langle 110 \rangle}$ ($K_2 > 0$, the cases E and F of §1 of Sec. I)

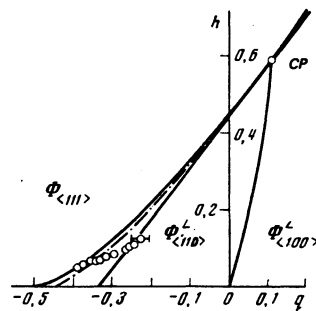


FIG. 7. Theoretical phase diagram for $H_0 \parallel \langle 111 \rangle$ ($K_2 > 0$) together with experimental data for the iron garnet $\text{Sm}_3\text{Fe}_5\text{O}_{12}$. Temperature range: 56–63 K. The mean values of the errors, not including the systematic measurement errors discussed in the text, are given.

on samarium-iron-garnet ($\text{Sm}_3\text{Fe}_5\text{O}_{12}$) samples are much smaller (down to $0.18M_0$). For this reason the anomalies in the magnetization curves of $\text{Sm}_3\text{Fe}_5\text{O}_{12}$ are more feebly marked, which leads to a reduction in the accuracy with which the transition fields can be determined. In Fig. 7 we show the theoretical orientation phase diagram for the transition $\Phi'_{\langle 110 \rangle} \rightleftharpoons \Phi_{\langle 111 \rangle}$ ($K_2 > 0$). The stability-loss and phase-equilibrium lines were computed from Eqs. (21)–(24). In the same figure we have plotted experimental points corresponding to the anomalies in the magnetization curves of monocrystalline spheres of $\text{Sm}_3\text{Fe}_5\text{O}_{12}$. It can be seen that, as q increases (the temperature decreases), the experimental data systematically deviate downwards from the phase-equilibrium curve. Apparently, the cause of this discrepancy is, besides the indicated reduction in the transition-field measurement accuracy, the substantial systematic errors made in the measurement of the fairly large magnetic-anisotropy constants of $\text{Sm}_3\text{Fe}_5\text{O}_{12}$ at $T < 77$ K in fields of moderate strength, something which is assumed in Ref. 27. For example, at $T = 56$ K the anisotropy constants, measured in a 10-kOe field, have the following values: $K_1 = -2 \times 10^6$ erg/cm³, $K_2 = 8.3 \times 10^6$ erg/cm³. To these constants correspond an anisotropy field $H_A = 33$ kOe, which is higher than the external field. In such a situation, the sample may turn out to be unsaturated in the difficult directions during the measurement of K_1 and K_2 by the torque method, and this will lead to systematic errors. Unfortunately, the variation range of the parameter q of the ferrite $\text{Sm}_3\text{Fe}_5\text{O}_{12}$ does not allow passage through the isolated CP and the investigation of the first-order transitions $\Phi'_{\langle 100 \rangle} \rightleftharpoons \Phi_{\langle 111 \rangle}$ and $\Phi'_{\langle 110 \rangle} \rightleftharpoons \Phi_{\langle 100 \rangle}$.

More favorable is the case of the investigation of the first-order transitions $\Phi'_{\langle 111 \rangle} \rightleftharpoons \Phi_{\langle 110 \rangle}$ ($K_2 > 0$, Fig. 1f), since this transition is investigated at higher temperatures, where the anisotropy constants have been measured more

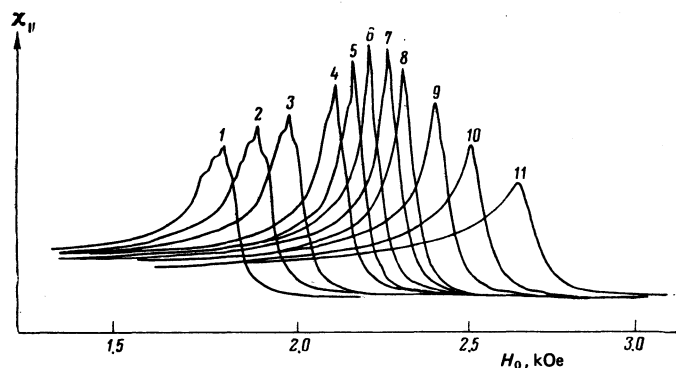


FIG. 8. Dependence of the differential susceptibility χ_H of the iron garnet $\text{Sm}_3\text{Fe}_5\text{O}_{12}$ on the external magnetic field intensity for the case of a spherical sample and $H_0 \parallel \langle 111 \rangle$. The curves were recorded in increasing fields at T K: 1) 68.3; 2) 71.3; 3) 71.8; 4) 72.3; 5) 72.5; 6) 72.6; 7) 72.8; 8) 73.0; 9) 73.3; 10) 73.6; 11) 74.2.

accurately, and, moreover, the variation range of q allows passage through the CP of first- and second-order transitions and the observation of a second-order transition. The phase diagram was constructed from the results of the study of the field dependences of the magnetic-susceptibility components χ_{\parallel} and χ_{\perp} . It is not difficult to deduce within the framework of the phenomenological approximation that in crossing a second-order phase-transition curve the component χ_{\perp} of an unbounded sample diverges, while χ_{\parallel} has a singularity, but that at the CP χ_{\parallel} also diverges.

In Fig. 8 we show experimental $\chi_{\parallel}(H_0)$ dependences, obtained on a monocrystalline sphere of $\text{Sm}_3\text{Fe}_5\text{O}_{12}$ for $H_0 \parallel \langle 110 \rangle$ in the temperature range 68–74 K. It can be seen that both the first- and the second-order phase transition are characterized by susceptibility peaks, although these peaks differ totally in character. In the case of the first-order transitions the χ_{\parallel} peak is mainly due to the DB-displacement processes that occur during the reconstruction of the domain structure in the intermediate state of the ferromagnet, i.e., to the redistribution of the phase volumes. This is indicated, for example, by the irregular kinks in the low-temperature $\chi_{\parallel}(H_0)$ dependences, kinks which are well reproduced in experiment after experiment. The cause of such irregularities may be the hindrance of the DB by the crystal defects. It is clear that a $\chi_{\parallel}(H_0)$ peak corresponds to a point of inflection of the dependence $\rho_{\langle 110 \rangle}(H_0)$, while the magnetic-field strength at the point of the peak can roughly be taken as the first-order phase-transition field. At the same time, the high-temperature $\chi_{\parallel}(H_0)$ dependences are smooth, and the magnetic field corresponding to a χ_{\parallel} peak can be regarded as a second-order phase-transition field. And, finally, since χ_{\parallel} diverges at the CP, while it has a maximum of finite height for $q \neq q_c$, we assumed that to the critical temperature should correspond to the $\chi_{\parallel}(H_0)$ dependence with the highest peak. The curve 6 in Fig. 8, which is consistent with this assumption, was used to determine the coordinates of the CP on the phase diagram.

The behavior of the susceptibility χ_{\perp} is similar, but from the $\chi_{\perp}(H_0)$ curves the coordinates of the CP can be determined with less accuracy, since the dependence of the height of the χ_{\perp} maximum on q is less critical. We can indicate two causes of such behavior of $\chi_{\perp}(H_0, q)$. First, $\chi_{\perp}(H_0)$ of an infinite crystal diverges not only at the CP, but everywhere on the second-order phase-transition curve. Secondly, the susceptibility χ_{\perp} vanishes when H_0 is precisely oriented along a $\langle 110 \rangle$ direction, since the contributions of the equivalent $\Phi_{\langle 111 \rangle}$ phase cancel out. Only when the field is inclined at an angle of several degrees to a $\langle 110 \rangle$ -type axis is it possible to measure a $\chi_{\perp}(H_0)$ dependence, but then the phase transition ceases to be a second-order transition.

In Fig. 9 we show the theoretical phase diagram [Eqs. (27) and (28)] and a number of experimental points obtained from the susceptibility anomalies. It can be seen that the agreement between the experimental data and the theoretical diagram is satisfactory, although the ordinate of the CP is smaller than its theoretical value by roughly 15%. The cause of such a discrepancy is, ap-

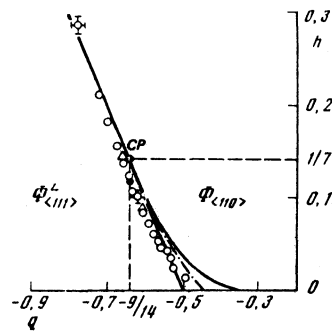


FIG. 9. Theoretical phase diagram for $H_0 \parallel \langle 111 \rangle$ ($K_2 > 0$) together with experimental data obtained for the ferrite $\text{Sm}_3\text{Fe}_5\text{O}_{12}$ from susceptibility measurements on a spherical sample: Δ) $\chi_{\parallel}(H_0)$ measurements; \circ) $\chi_{\perp}(H_0)$ measurements; \bullet) critical point obtained from the family of $\chi_{\perp}(H_0, q)$ curves. Temperature range: 68–74 K. Typical measurement errors are shown.

parently, the above-discussed inaccuracy of the measurement of the anisotropy constants and the influence of the susceptibility of the para-process.

CONCLUSION

The above-performed theoretical investigations of the spin-reorientation phase diagrams of a cubic ferromagnet in a magnetic field have revealed a wide variety of magnetic phase transitions. The appreciable effect of the transitional domain structure on the character of first-order SFPT in samples of finite dimensions has been elucidated. Experimental magnetization, susceptibility, and NMR investigations on iron garnets have confirmed the results of the theory.

The authors are grateful to B. V. Mill' and A. G. Titova for growing the iron-garnet single crystals, as well as to S. F. Ivanov for his help in the measurements.

¹ Allowance for the third anisotropy constant (i.e., for the eighth-order term) eliminates this inconsistency, but leads to a significant complication of the situation: in zero field, besides the enumerated phases, which correspond to the orientation of \mathbf{M} along the principal directions of the type $\langle 100 \rangle$, $\langle 111 \rangle$, and $\langle 110 \rangle$, angular phases for which \mathbf{M} lies in planes of the type $\langle 110 \rangle$ and $\langle 100 \rangle$ can also be realized. [2, 8, 20] Since the magnitude of the constant K_3 is appreciable only for a limited number of cubic ferromagnets and allowance for the eighth-order term in the expression for f_A leads, for $H \neq 0$, to extremely unwieldy and complicated results, we carried out the investigation of SFPT in a magnetic field within the framework of the model with two anisotropy constants.

¹ K. P. Belov, A. K. Zvezdin, A. M. Kadomtseva, and R. Z. Levitin, Usp. Fiz. Nauk 119, 447 (1976) [Sov. Phys. Usp. 19, 574 (1976)].

² K. P. Belov, A. K. Zvezdin, R. Z. Levitin, A. S. Markosyan, B. V. Mill', A. A. Mukhin, and A. P. Perov, Zh. Eksp. Teor. Fiz. 68, 1190 (1975) [Sov. Phys. JETP 41, 590 (1975)].

³ G. Chandra and T. S. Radhakrishnan, Phys. Lett. 28A, 323 (1968).

⁴ V. D. Doroshev, S. F. Ivanov, N. M. Kovtun, and V. N. Seleznev, Dokl. Akad. Nauk Ukr. SSR Ser. A, No. 1, 68 (1973).

⁵ V. A. Borodin, V. D. Doroshev, V. A. Klochan, N. M. Kovtun, R. Z. Levitin, and A. S. Markosyan, Zh. Eksp. Teor. Fiz. 70, 1363 (1976) [Sov. Phys. JETP 43, 711 (1976)].

⁶ V. A. Borodin, V. D. Doroshev, V. A. Klochan, N. M. Kovtun,

- and A. G. Titova, *Fiz. Tverd. Tela (Leningrad)* **18**, 1852 (1976) [*Sov. Phys. Solid State* **18**, 1080 (1976)].
- ⁷U. Atzmony, M. P. Dariel, E. R. Bauminger, D. Lebenbaum, I. Nowik, and S. Ofer, *Phys. Rev. B* **7**, 4220 (1973).
- ⁸U. Atzmony and M. P. Dariel, *Phys. Rev. B* **10**, 2060 (1974); **B13**, 4006 (1976).
- ⁹J. Sznajd and J. Klamut, *Acta Phys. Pol.* **A45**, 755 (1974).
- ¹⁰J. Sznajd, *Acta Phys. Pol.* **A47**, 61 (1975).
- ¹¹D. Mukamel, E. Domany, and M. E. Fisher, *Proc. Intern. Conf. on Magnetism, ICM-76, Amsterdam*, publ. in: *Physica (Utrecht) B+C*, **86-88**, 572 (1977).
- ¹²N. S. Akulov, *Ferromagnetizm (Ferromagnetism)*, Gostekhizdat, 1939.
- ¹³A. I. Belyaeva, V. V. Eremenko, V. N. Pavlov, and A. V. Antonov, *Zh. Eksp. Teor. Fiz.* **53**, 1879 (1967) [*Sov. Phys. JETP* **26**, 1069 (1968)].
- ¹⁴A. I. Belyaeva, R. A. Vaishnoras, V. V. Eremenko, V. I. Silaev, and Yu. N. Stel'makhov, *Fiz. Nizk. Temp.* **1**, 353 (1975) [*Sov. J. Low Temp. Phys.* **1**, 175 (1975)].
- ¹⁵L. Neel, *J. Phys. Radium* **5**, 241, 265 (1944).
- ¹⁶R. R. Birss and B. C. Hegarty, *Br. J. Appl. Phys.* **17**, 1241 (1966).
- ¹⁷E. C. Stoner, *Rep. Prog. Phys.* **13**, 83 (1950).
- ¹⁸V. G. Bar'yakhtar, A. E. Borovik, and V. A. Popov, *Pis'ma Zh. Eksp. Teor. Fiz.* **9**, 634 (1969); *Zh. Eksp. Teor. Fiz.* **62**, 2233 (1972) [*JETP Lett.* **9**, 391 (1969); *Sov. Phys. JETP* **35**, 1169 (1972)].
- ¹⁹V. G. Bar'yakhtar and V. A. Popov, *Problemy fiziki tverdogo tela*, Tr. Instituta fizika metallov (Problems of Solid State Physics: Transactions of the Institute of Metal Physics), No. 31, Urals Science Center, Sverdlovsk, 1975, p. 186.
- ²⁰R. R. Birss, G. R. Evans, and D. J. Martin, *Proc. Intern. Conf. on Magnetism, ICM-76, Amsterdam*, publ. in: *Physica (Utrecht) B+C*, **86-88**, 1371 (1977).
- ²¹A. Z. Patashinskiĭ and V. L. Pokrovskii, *Fluktuatsionnaya teoriya fazovykh perekhodov (The Fluctuation Theory of Phase Transitions)*, Nauka, 1975, p. 30.
- ²²K. P. Belov, A. K. Gapeev, R. Z. Levitin, A. S. Markosyan, and Yu. F. Popov, *Zh. Eksp. Teor. Fiz.* **68**, 241 (1975) [*Sov. Phys. JETP* **41**, 117 (1975)].
- ²³N. M. Kolacheva, R. Z. Levitin, and L. P. Shlyakhina, *Fiz. Tverd. Tela (Leningrad)* **19**, 970 (1977) [*Sov. Phys. Solid State* **19**, 565 (1977)].
- ²⁴V. G. Demidov, R. Z. Levitin, and Yu. F. Popov, *Fiz. Tverd. Tela (Leningrad)* **18**, 596 (1976) [*Sov. Phys. Solid State* **18**, 347 (1976)].
- ²⁵C. Robert and F. Hartmann-Boutron, *J. Phys. Radium* **23**, 574 (1962).
- ²⁶R. L. Streever and P. J. Caplan, *Phys. Rev.* **B4**, 2881 (1971).
- ²⁷E. J. Heilner and W. H. Grodkiewicz, *AIP Conf. Proc.*, No. 18, *Magnetism and Magnetic Materials*, 1973, p. 1232.

Translated by A. K. Agyei

Exchange interaction mechanisms in magnetic semiconductors

A. N. Kocharyan and P. S. Ovnanyan

Erevan Physics Institute

(Submitted 7 July 1977)

Zh. Eksp. Teor. Fiz. **74**, 620-628 (February 1978)

Effective exchange interaction in magnetic semiconductors is deduced by taking into account various factors: hybridization of the f -electron states with the valence and conduction bands, total interatomic exchange including the interband interaction of the electrons, Coulomb repulsion effect, and the effect of the finite f -level width. The calculated values of the exchange constants I_1 and I_2 for europium chalcogenides are in good agreement with the experimental values.

PACS numbers: 75.30.Et

1. In the description of the properties of magnetic dielectrics and semiconductors based on transition and rare-earth metals (REM), various mechanisms of exchange interaction are resorted to. Whereas the Kramers superexchange interaction mechanism^[1] suffices to explain the magnetism of magnetic dielectrics, which are antiferromagnetic in most cases, the situation is more complicated in the case of magnetic semiconductors based on REM. Thus, for example, in the series of europium-chalcogenides, which have a more complicated electronic structure, one observes a broad spectrum of magnetic properties on going from compound to compound or when the lattice parameter is altered by pressure.^[2,3] Xavier and de Graaf^[4,5] attempted to explain both the ferromagnetic and antiferromagnetic exchange interactions in EuO and EuS by using only the Bloembergen-Rowland interband-interaction mechanism.^[6] Their overstated values of the interband-interaction constants can, however, not be regarded as acceptable.

An analogous mechanism, due to excitation of electrons from localized p orbits of anions into the conduction band, was proposed by Berdyshev and Letfulov^[7] and by Kazakov.^[8] The data they used, however, were taken from experimental papers^[9,10] whose authors incorrectly identified the forbidden gap width B with the f -level^[1] binding energy Δ . The real values of the parameters B (see Table I) in europium chalcogenides are 2-6 times larger than those assumed in the aforementioned theoretical papers,^[7,8] so that the obtained exchange integrals are smaller by one or two orders of magnitude than those given in Table II of ^[7]. Thus, the interband-interaction mechanism alone is not sufficient to obtain good agreement with the experimental data.

It follows from magneto-optical measurements and from calculations of the band structure with allowance for the strong f -electron correlation^[12] and the lattice polarization^[13] that in europium chalcogenides the localized weakly smeared f level lies in the forbidden gap